Environmental Science
Water Research & Technology

ROYAL SOCIETY
OF CHEMISTRY

PAPER
Jiahai Ma *et al.*
Strongly enhanced persulfate activation by bicarbonate
accelerated Cu(III)/Cu(I) redox cycles

ROYAL SOCIETY OF CHEMISTRY

PAPER

Check for updates

Strongly enhanced persulfate activation by bicarbonate accelerated Cu(III)/Cu(I) redox cycles†

Jun Zhang, Shenjun Wang, Yuhao Wu and Jiahai Ma [iD] *

In advanced oxidation systems, the promoting effect of bicarbonate is relatively overlooked. Bicarbonate, as an inorganic anion widely present in natural waters, is extremely important for water treatment. Therefore, bicarbonate was added to a PDS/Cu^{2+} system to investigate the degradation mechanisms of organic contaminants. The generation of alkyl radicals in the PDS/Cu^{2+}/HCO$_3^-$ system was first demonstrated through Electron Paramagnetic Resonance (EPR) testing. This study reveals that the introduced bicarbonate ions undergo transformation into alkyl radicals. The presence of alkyl radicals promotes the cycling of monovalent, divalent, and trivalent copper ions, facilitating the degradation of contaminants. The production of monovalent and trivalent copper ions in the reaction system was confirmed through UV-vis absorption spectroscopy and quenching experiments. Furthermore, the change in the oxidation state of copper ions was further confirmed through EPR testing. These findings not only shed new light on the degradation mechanism of the PDS/Cu^{2+} system in the presence of bicarbonate but also open up new avenues for the further application of bicarbonate in advanced oxidation processes.

Water impact

Persulfate-based AOPs for the treatment of pollutants have attracted considerable attention, but the reaction mechanisms involved are complex and controversial. In this study, the bicarbonate ion, an inorganic anion prevalent in natural waters, is introduced to the PDS/Cu^{2+} system to degrade refractory azo compounds. It is found that the PDS/HCO$_3^-$/Cu^{2+} system produces monovalent copper ions and trivalent copper ions. Moreover, alkyl radicals are captured in this system. Therefore, we deduce that bicarbonate is converted to alkyl radicals, which facilitate the cycling of copper ions in different valence states, thus promoting target degradation. The results could provide new designs and insights into persulfate-based AOPs.
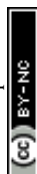
1. Introduction

The current water pollution problem is a serious global challenge. And the wastewater from industrial production contains large amounts of organic pollutants that have significant impacts on human health, ecosystems, and sustainable development.[1,2] Therefore, it is essential to develop highly efficient technologies to address water pollution issues. Currently, advanced oxidation processes (AOPs) are considered one of the most efficient techniques for eliminating organic contaminants.[3] Persulfate-based AOPs have gained significant attention due to the production of sulfate radicals (SO$_4^{\cdot-}$) and their robust oxidizing capability (E = 2.5–3.1 V) over a wide pH range.[4–6] Common methods of activating persulfate include the use of heat, UV irradiation, visible light, ultrasound, transition metal ions[7–9] and other

catalysts.[10–12] Compared with energy-based methods, the introduction of transition metal ions not only reduces energy consumption but also minimizes potential side reactions and unwanted by-products, making it a more energy-efficient and economical method. Iron ions (Fe^{2+}/Fe^{3+}), cobalt ions (Co^{2+}), copper ions (Cu^{2+}) and manganese ions (Mn^{2+}) are typically used for the activation of persulfate.[13–17]

Recently, copper ions have attracted more attention in AOPs. Copper ions exhibit a desirable level of reactivity with persulfate, generating reactive sulfate radicals. The selection of copper ions as an activator for PDS offers a balance between reactivity, stability, compatibility, and environmental considerations. However, in homogeneous systems, most applications of Cu^{2+} are under acidic or neutral conditions, even under heating conditions and requiring longer reaction times.[18,19] In addition, adding other metal ions or chemical reduction reagents is also a common method to facilitate the cycling of copper ions to activate persulfate.[20] Common reduction reagents include hydroxylamine, L-ascorbic acid[21] and cysteine.[22] However, the external addition of energy, heat and reducing agents will increase costs and even cause

School of Chemical Sciences, University of Chinese Academy of Sciences, Beijing 100049, P. R. China. E-mail: majia@ucas.ac.cn

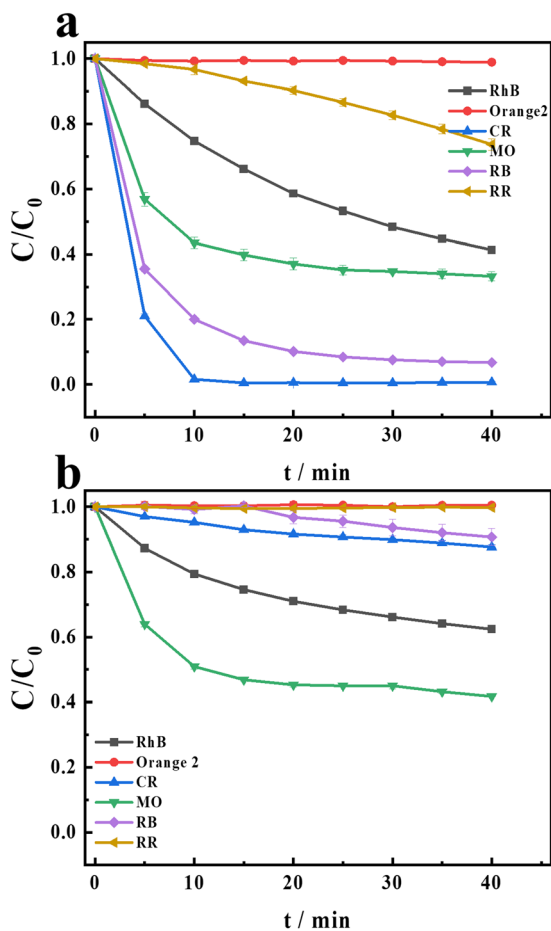† Electronic supplementary information (ESI) available. See DOI: https://doi.org/10.1039/d4ew00172a

This journal is © The Royal Society of Chemistry 2024

Environ. Sci.: Water Res. Technol., 2024, **10**, 1785–1794 | 1785

Fig. 1 The degradation of the different compounds in (a) PDS/Cu²⁺/HCO₃⁻ and (b) PDS/Mn²⁺/HCO₃⁻ systems. [PDS] = 16 mM, [NaHCO₃] = 20 mM, [Cu²⁺] = 0.1 mM, [Mn²⁺] = 0.1 mM, and [CR] = [RhB] = [RR] = [RB] = [MO] = [Orange 2] = 0.02 mM.

secondary pollution. As a widely existing inorganic anion present in natural waters, most studies point out that bicarbonate plays a negative role, and it is typically believed to quench free radicals in AOPs.[23] However, recently, some studies have found that the addition of bicarbonate can drive Fenton-like reactions. For example, Yang *et al.*[24] found that after adding HCO₃⁻ into a H₂O₂/Cu²⁺ system, Congo red could be effectively degraded. Jiang *et al.*[25] found that HCO₃⁻ could activate PDS and generate HCO₄⁻ to degrade acetaminophen. There will be the formation of carbonate radical anions in the oxidation of iron by oxygen in the presence of HCO₃⁻. In addition, it has been found that HCO₃⁻ can also promote the activation of peroxides with a heterogeneous catalyst by inhibiting the leaching of metal ions in the heterogeneous catalyst, thus enhancing the degradation of pollutants.[26,27]

Interestingly, in our study, HCO₃⁻ can promote the degradation of Congo red (CR), a recalcitrant contaminant containing azo bonds, in the PDS/Cu²⁺ system. The catalysis of Cu²⁺ under alkaline conditions is rarely mentioned. In this study, a weak alkaline condition is created by introducing bicarbonate into the PDS/Cu²⁺ system. After adding HCO₃⁻, CR can be almost completely

degraded in 40 minutes. In order to clarify the reaction mechanisms, we carried out a series of experiments. CR is selected as the target pollutant to evaluate the performance of the PDS/Cu²⁺/HCO₃⁻ system. Firstly, when adding HCO₃⁻ into PDS/Cu²⁺ and PDS/Mn²⁺ systems, respectively, CR can be completely degraded in the PDS/Cu²⁺/HCO₃⁻ system, while CR cannot be degraded at all in the PDS/Mn²⁺/HCO₃⁻ system, demonstrating that HCO₃⁻ can selectively improve the reaction activity of Cu²⁺. Through chromogenic reactions and electron paramagnetic resonance, the production of Cu(III) and Cu(I) in the PDS/Cu²⁺/HCO₃⁻ system is demonstrated. In addition to the production of Cu(III) and Cu(I), alkyl radicals are captured after adding HCO₃⁻. Therefore, we propose that in the PDS/Cu²⁺/HCO₃⁻ system, alkyl radicals will form, accelerating the cycling of copper ions and completely degrading contaminants. This finding overturned previous studies that HCO₃⁻ can inhibit AOPs.[28] Our study provides new insights into persulfate-based Fenton-like reactions.

2. Materials and methods

2.1. Materials and reagents

Potassium persulfate (PDS) is purchased from Meryer. Potassium monopersulfate triple salt (PMS) and sodium bicarbonate (NaHCO₃) are purchased from Aladdin. Anhydrous sodium carbonate (Na₂CO₃) is purchased from Sinopharm Chemical Reagent. Copper chloride dihydrate (CuCl₂) is purchased from Alfa Aesar; manganese chloride tetrahydrate (MnCl₂), methylene blue hydrate (MB), furfuryl alcohol (FFA), hydroxylammonium chloride (NH₂OH·HCl), iron chloride hexahydrate (FeCl₃), sodium chloride (NaCl), sodium dihydrogen phosphate (NaH₂PO₄), reactive red 195 (RR), methanol (MeOH), sodium periodate (NaIO₄) and *tert*-butanol (TBA) are purchased from Macklin. Congo red (CR) is purchased from TCI. Deuterium oxide (D₂O) is purchased from Damas-Beta. Rhodamine B (RhB) is purchased from Amresco. Trichloromethane (CHCl₃) is purchased from Beijing Chemical Works. All chemicals are of analytical grade.

2.2. Reaction procedures

The degradation experiments are conducted in a 50 mL beaker, stirring at 700 rpm, at room temperature and pressure. The pH is not adjusted in this experiment, except for discussing the influence of pH on the degradation of CR. First, the CR solution is added into the beaker, and then NaHCO₃, CuCl₂, and other solutions are added. Finally, PDS is added to trigger the reaction. At specific time intervals, a 3 mL sample solution is collected and injected into a quartz cuvette to measure the degradation of the contaminants. NaOH and HCl are used to adjust the pH when evaluating the effect of pH values. To investigate the effect of reactive oxygen species (ROS), methanol (MeOH) and *tert*-butanol (TBA) are used to scavenge HO˙ and SO₄˙⁻, furfuryl alcohol (FFA) as an ¹O₂ scavenger, and
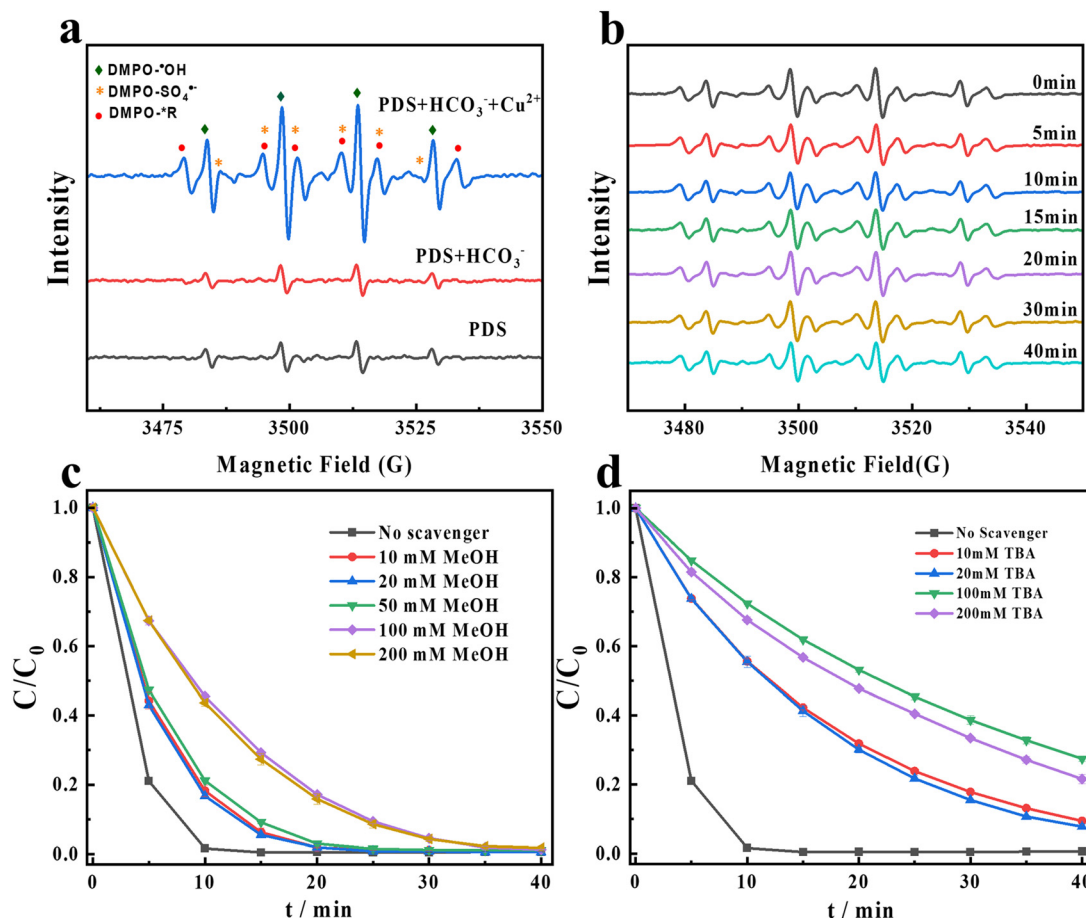
1786 | *Environ. Sci.: Water Res. Technol.*, 2024, **10**, 1785–1794

This journal is © The Royal Society of Chemistry 2024

Fig. 2 (a) EPR spectra for the degradation of CR in different systems. (b) The changes of EPR signals at different times in the PDS/Cu^{2+}/HCO$_3^-$/CR system. Degradation efficiency for CR after adding (c) MeOH and (d) TBA. Experimental conditions: [PDS] = 16 mM, [NaHCO$_3$] = 20 mM, [Cu^{2+}] = 0.1 mM, and [CR] = 0.02 mM.

chloroform (CHCl$_3$) as an O$_2^{\bullet-}$ scavenger. The selectivity of the PDS/Cu^{2+}/HCO$_3^-$ system is demonstrated by comparing the degradation of different contaminants. Neocuproine (NCP) is used to demonstrate the presence of Cu(I), and periodate (PI) is used to demonstrate the presence of Cu(III).

2.3. Analysis

The degradation of CR, RhB, MO, RB, RR, and Orange 2 is analyzed with an ultraviolet-visible (UV) spectrophotometer (TU-1900). Different active species were tested by electron paramagnetic resonance (EPR) (EMXplus, Bruker, Germany). Relevant parameters are as follows: a center field of 3517.3 G, a sweep time of 30 s, and a microwave power of 20 dB. The presence of Cu(I) is measured spectrophotometrically using NCP; the UV absorbance of the complex formed by Cu(III) and NaIO$_4$ can be detected at 450 nm. The 3D fluorescence spectra were collected with a fluorescence spectrophotometer (HORIBA. EDISON, NJ, USA). The change of the functional groups of CR before and after degradation was analyzed by Fourier-transform infrared spectroscopy (Bruker, Germany).

3. Results and discussion

3.1. Degradation activity

Previous research[24] has demonstrated that the H$_2$O$_2$/Cu^{2+}/HCO$_3^-$ system exhibits higher excellent degradation performance than the H$_2$O$_2$/Mn^{2+}/HCO$_3^-$ system in the degradation of CR. Recently, persulfate-based AOPs have attracted more attention in treating organic contaminants.[29–31] Therefore, persulfate (PDS) is chosen as the oxidant in this research. Firstly, in order to evaluate the degradation performance of the PDS/Cu^{2+}/HCO$_3^-$ and PDS/Mn^{2+}/HCO$_3^-$ systems, six dyes are chosen as target contaminants. These six dyes are stable and can hardly be degraded in the natural environment. The structures of the six dyes are shown in Scheme S1.† The two systems exhibited different degradation efficiencies for the dyes as illustrated in Fig. 1. Compared with the PDS/Mn/HCO$_3^-$ system, the PDS/Cu^{2+}/HCO$_3^-$ system exhibits a better degradation efficiency. The difference in the degradation of CR between these two systems is the most pronounced. In the PDS/Mn^{2+}/HCO$_3^-$ system, the degradation of CR is almost negligible, while in the PDS/Cu^{2+}/HCO$_3^-$ system, CR is almost completely degraded. Therefore, CR, a representative azo dye,
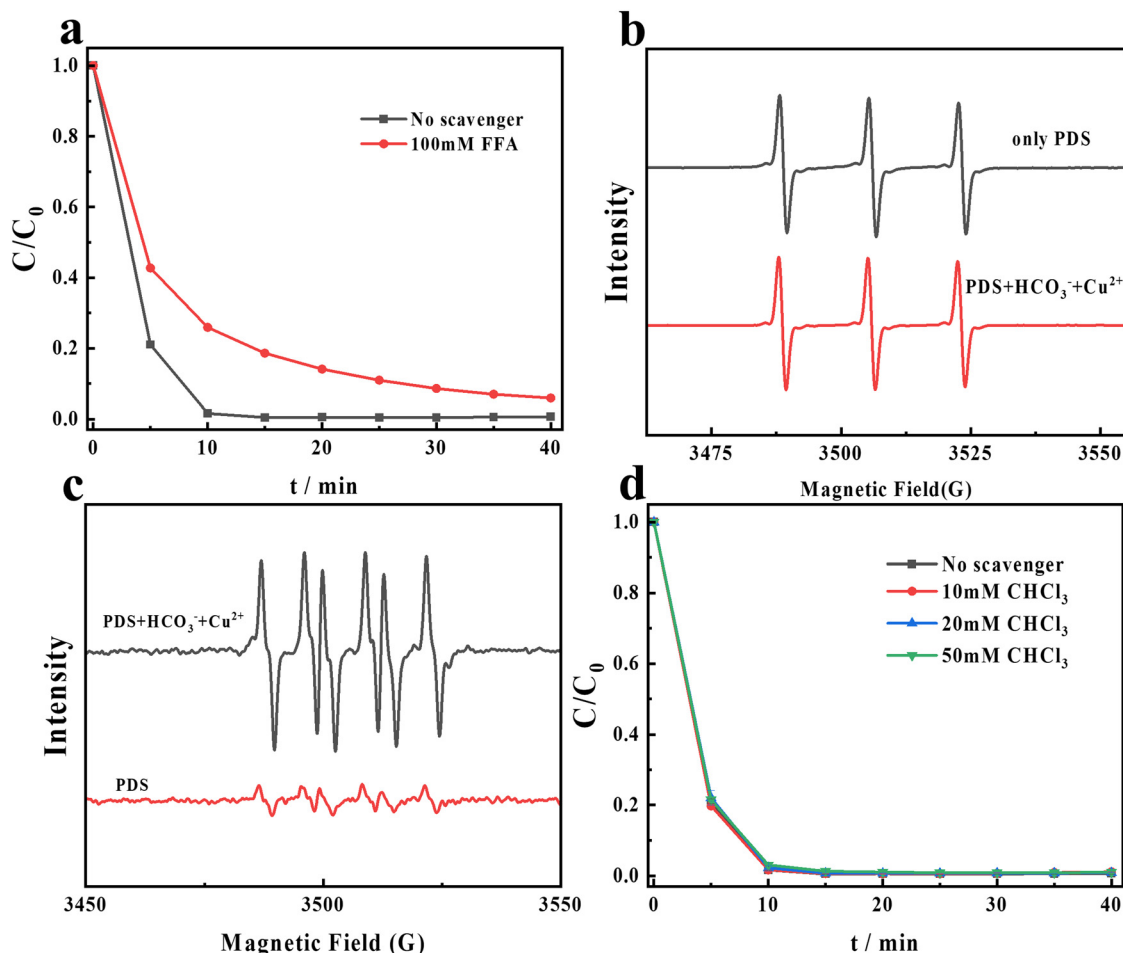
This journal is © The Royal Society of Chemistry 2024

Environ. Sci.: Water Res. Technol., 2024, **10**, 1785–1794 | **1787**

Fig. 3 (a) Effects of FFA on CR degradation in the PDS/HCO_3^-/Cu^{2+} system; (b) the EPR spectra of CR degradation in different systems (PDS + H_2O; PDS + $NaHCO_3$ + $CuCl_2$ + H_2O). (c) The EPR spectra of CR degradation in different systems (PDS + DMSO; PDS + $NaHCO_3$ + $CuCl_2$ + DMSO). (d) Effects of different concentrations of $CHCl_3$ on CR degradation by the PDS/HCO_3^-/Cu^{2+} system. Experimental conditions: [PDS] = 16 mM, [$NaHCO_3$] = 20 M, [Cu^{2+}] = 0.1 M, and [CR] = 0.02 M.

is selected as the model compound to assess the degradation activity of the PDS/HCO_3^-/Cu^{2+} system. Further experiments are conducted to explore the mechanisms involved in the PDS/Cu^{2+}/HCO_3^-/CR system. Fig. S1† shows the degradation of CR under different conditions. It is obvious that CR cannot be degraded in PDS, PDS/HCO_3^-, and PDS/Cu^{2+} systems, and the degradation efficiency can be up to 99.3% in the PDS/HCO_3^-/Cu^{2+}system, indicating that the addition of HCO_3^- significantly promotes the reaction.

3.2. Identification of ROS

3.2.1. Identification of HO˙, $SO_4^{˙-}$ and alkyl radicals. $SO_4^{˙-}$ and HO˙ are two common free radicals in persulfate-based AOPs (eqn (1)–(3)).[4,32] In order to identify whether $SO_4^{˙-}$ and HO˙ exist in the PDS/Cu^{2+}/HCO_3^-/CR system, EPR tests are conducted using DMPO as the trapping agent.

As shown in Fig. 2a, a quartet signal with an intensity ratio of 1:2:2:1 can be observed in both the sole PDS system and the PDS/HCO_3^- system. This signal, with A_N = 15.0 (G) and A_H = 14.7 (G), is assigned to DMPO–HO˙. After adding Cu^{2+} to the

PDS/HCO_3^- system, the EPR signals change significantly. In addition to the marked enhancement of HO˙, $SO_4^{˙-}$ is obviously produced. In addition, another new radical signal with A_N = 15.7 G and A_H = 22.5 G is generated in the PDS/Cu^{2+}/HCO_3^-/CR system. Based on the hyperfine coupling constants, the new signal can be considered as alkyl radicals. Being the only carbon-containing species in the system, the alkyl radicals should be derived from bicarbonate. In the presence of sulfate radicals, bicarbonate can be firstly converted to carbonate radicals (eqns (4) and (5)),[33] and further converted to alkyl radicals. We proposed several pathways for generating alkyl radicals: (1) PDS, as an oxidant, can react with bicarbonate, initiating a single-electron transformation process, leading to the formation of carbonate radicals, and then generating alkyl radicals under the catalysis of copper ions; (2) the monovalent or divalent copper ions generated in this system can form a complex with carbonate radicals. Subsequently, the complex undergoes an electron transfer process to form alkyl radicals; (3) the trivalent copper ions produced in this system exhibit strong oxidizing properties in aqueous solution and may undergo an oxidation reaction with carbonate radicals, leading
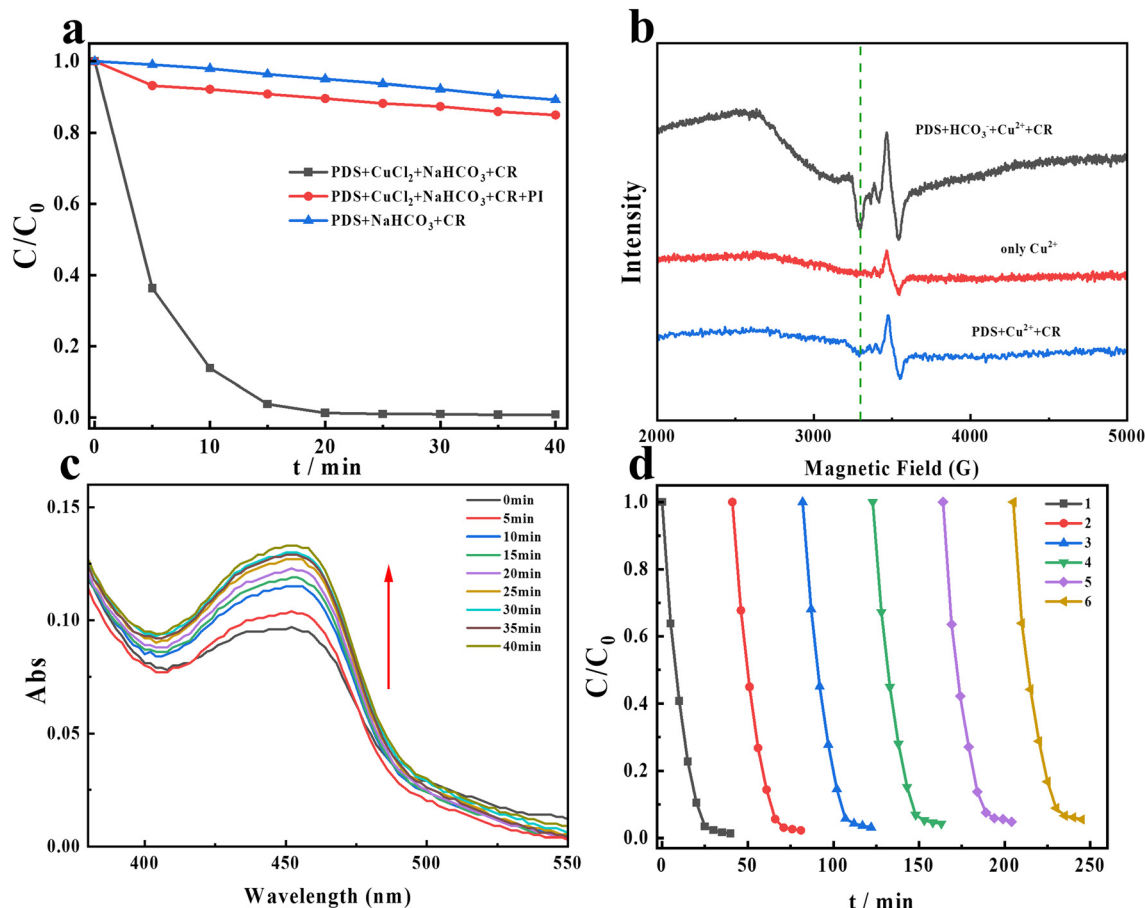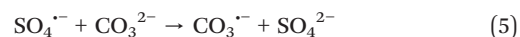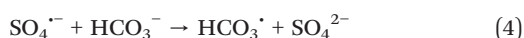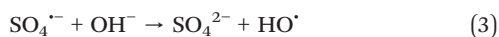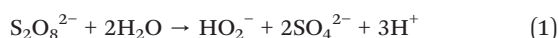
Fig. 4 (a) The degradation of CR after the addition of NaIO$_4$; (b) EPR signals of the new copper species at different systems; temperature is 90 K; (c) the absorbance of the complex of copper and NCP after adding PDS and HCO$_3^-$ at different times; (d) the reusability of Cu^{2+} on CR degradation in the PDS/HCO$_3^-$/Cu^{2+} system. Experimental conditions: [PDS] = 16 mM, [NaHCO$_3$] = 20 mM, [Cu^{2+}] = 0.1 mM, [NaIO$_4$] = 10 mM, and [CR] = 0.02 mM.

to the loss of one electron from an oxygen atom on the carbonate radical and the formation of the alkyl radicals. Hence, we can deduce that the signal of the newly generated carbon-centered radical is an alkyl radical in Fig. 2a. In order to further evaluate the role of radicals, MeOH is chosen as the scavenger of both SO$_4^{\bullet-}$ and HO$^\bullet$ ($K_{OH,MeOH} = 1.2 \times 10^9$ M^{-1} S^{-1} and $K_{SO_4^{\bullet-},MeOH} = 1.6 \times 10^7$ M^{-1} S^{-1}), and TBA is chosen as the scavenger of HO$^\bullet$ ($K_{OH,TBA} = 6 \times 10^8$ M^{-1} S^{-1} and $K_{SO_4^{\bullet-},TBA} = 4 \times 10^5$ M^{-1} S^{-1}).[34,35] As shown in Fig. 2c, 99.3% of CR is degraded when no scavenger is added, while 98.2% of CR is degraded when 200 mM MeOH is added. As shown in Fig. 2d, 78.4% of CR is degraded when 200 mM TBA is added. Hence, SO$_4^{\bullet-}$ and HO$^\bullet$ play a relatively minor role in the degradation of CR, and they are not the ROS.

$$S_2O_8^{2-} + 2H_2O \rightarrow HO_2^- + 2SO_4^{2-} + 3H^+ \tag{1}$$

$$S_2O_8^{2-} + HO_2^- \rightarrow SO_4^{\bullet-} + 2SO_4^{2-} + H^+ + O_2^{\bullet-} \tag{2}$$

$$SO_4^{\bullet-} + OH^- \rightarrow SO_4^{2-} + HO^\bullet \tag{3}$$

$$SO_4^{\bullet-} + HCO_3^- \rightarrow HCO_3^\bullet + SO_4^{2-} \tag{4}$$

$$SO_4^{\bullet-} + CO_3^{2-} \rightarrow CO_3^{\bullet-} + SO_4^{2-} \tag{5}$$

$$2O_2^{\bullet-} + 2H_2O \rightarrow H_2O_2 + 2OH^- + {}^1O_2 \tag{6}$$

3.2.2. Identification of ${}^1O_2$ and O$_2^{\bullet-}$. Previous studies have reported that singlet oxygen (${}^1O_2$) and superoxide radicals (O$_2^{\bullet-}$) can be produced in persulfate-based AOPs, and they are considered reactive oxygen species.[36–38] In order to evaluate the impact of ${}^1O_2$ and O$_2^{\bullet-}$ in the PDS/HCO$_3^-$/Cu^{2+} system, EPR tests and quenching experiments are conducted. FFA is used as the scavenger of ${}^1O_2$ and HO$^\bullet$.[39,40] From Fig. 3a, the CR degradation decreased by 5% after adding 100 mM FFA. From the previous experimental results, we can find that the system is capable of producing HO$^\bullet$, so the FFA quenching experiment alone is inefficient to explain the role of ${}^1O_2$ in the system.

In order to further evaluate the role of ${}^1O_2$ in the PDS/HCO$_3^-$/Cu^{2+} system, EPR tests were conducted. From Fig. 3b, a triplet peak appeared, which can be assigned to a 2,2,6,6-tetramethyl-4-piperidinol-N-oxyl radical (1:1:1) triplet, confirming the presence of ${}^1O_2$ in a separate PDS system. The EPR signal intensity did not improve after the addition of Cu^{2+} and HCO$_3^-$ to the PDS system. It can be seen from Fig. S1† that the PDS
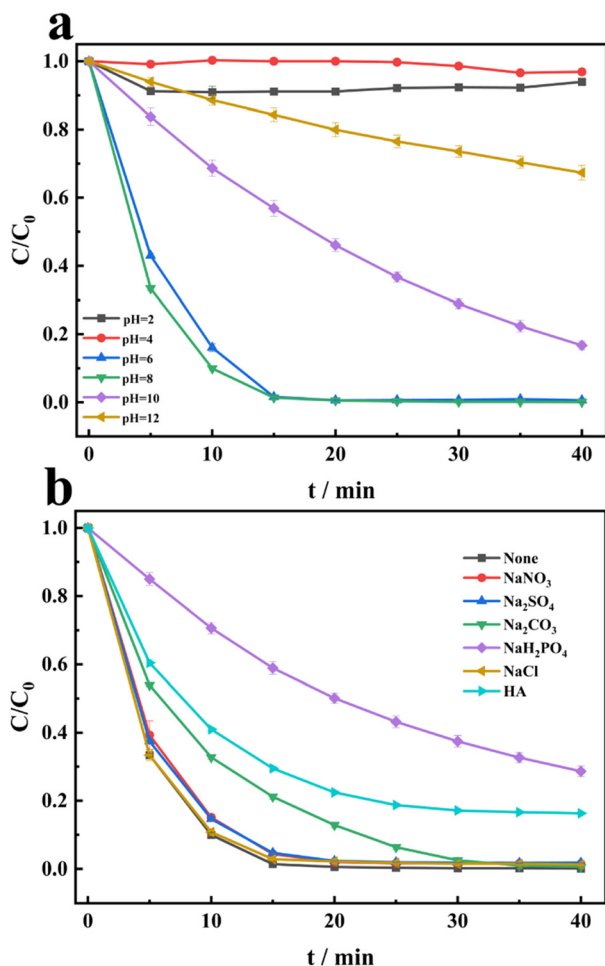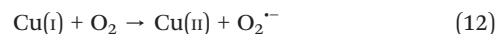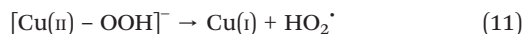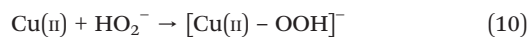
This journal is © The Royal Society of Chemistry 2024

Environ. Sci.: Water Res. Technol., 2024, **10**, 1785–1794 | **1789**

Fig. 5 (a) Effects of the initial pH on the degradation of CR in the PDS/HCO$_3^-$/Cu^{2+} system. (b) Effects of NO$_3^-$, SO$_4^{2-}$, CO$_3^{2-}$, H$_2$PO$_4^-$, Cl$^-$ and HA in the degradation of CR in the PDS/Cu^{2+}/HCO$_3^-$ system. [NO$_3^-$] = [SO$_4^{2-}$] = [CO$_3^{2-}$] = [H$_2$PO$_4^-$] = [Cl$^-$], [HA] = 10 mg L^{-1}, [CO$_3^{2-}$] = [H$_2$PO$_4^-$] = [Cl$^-$] = 10 mM, [HA] = 10 mg L^{-1}.

system alone was not able to effectively degrade CR. Therefore, we conclude that ^{1}O$_2$ is not the ROS degrading CR in the PDS/HCO$_3^-$/Cu^{2+} system. Accordingly, the lifetime of ^{1}O$_2$ in D$_2$O (20–32 μs) is more than 10-fold longer than that in H$_2$O (2 μs).[41] As shown in Fig. S2,† the efficiency of the degradation of CR did not increase in D$_2$O. The generation of ^{1}O$_2$ during the PDS activation process might be attributed to the presence of the superoxide anion O$_2^{•-}$ (eqn (6)).[42] From Fig. 4c, six-fold peaks of O$_2^{•-}$ are generated when using DMSO as the solvent. After adding HCO$_3^-$ and Cu^{2+}, the signal of DMPO–O$_2^{•-}$ significantly enhances. In order to further explore the role of O$_2^{•-}$ in this system, CHCl$_3$ is utilized as the scavenger of O$_2^{•-}$ ($K_{O_2^{•-},CHCl_3}$ = 1 × 10^9 M^{-1}S^{-1}).[43] However, after adding different concentrations of CHCl$_3$ into the PDS/HCO$_3^-$/Cu^{2+} system as shown in Fig. 3d, the degradation of CR has not been affected at all, indicating that O$_2^{•-}$ is not the ROS in the degradation of CR.

3.2.3. The cycling of Cu(ɪ) and Cu(ɪɪɪ). Through the above experiments, we deduce that free radicals and singlet oxygen are not the ROS on CR degradation in the PDS/HCO$_3^-$/Cu^{2+} system. Previous studies have mentioned that high-valent

metal species may play an important role in AOPs.[44–46] Recent studies have indicated that Cu(ɪɪɪ) could exist under neutral and alkaline conditions and is considered the dominant oxidant in contaminant degradation.[47,48] Reports demonstrate that Cu(ɪɪɪ) can be formed through several pathways (eqns (7)–(9)).[49,50] While Cu(ɪɪɪ) has a high oxidation capacity and may potentially act as an oxidant for contaminant oxidation, there is currently a lack of direct evidence to conclusively demonstrate its specific contribution in this regard. In addition, Cu(ɪɪɪ) cannot exist stably in aqueous solution. NaIO$_4$ is generally used to detect the presence of Cu(ɪɪɪ) because it is usually used as a scavenger to assess the contribution of Cu(ɪɪɪ). Additionally, it can react with Cu(ɪɪɪ) to form a complex that can be detected at 417 nm in the UV-visible spectrum.[16,51] As seen in Fig. 4a, in the presence of NaIO$_4$, the degradation of CR was significantly inhibited, and only 14% of CR can be degraded. Hence, it can be demonstrated that Cu(ɪɪɪ) is the dominant active species. Interestingly, obvious absorbance at 417 nm was observed in the PDS/HCO$_3^-$/Cu^{2+} system as shown in Fig. S3.† In addition, EPR tests were performed at a low temperature to investigate the changes in the valence of copper ions. From Fig. 4b, after adding PDS into the copper ion solutions, a new weak signal appears in the EPR spectra. Furthermore, with the continuous addition of HCO$_3^-$, the intensity of the new signal increases dramatically. Combining Fig. 4a and b, we further demonstrate that Cu(ɪɪɪ) was produced, and the addition of HCO$_3^-$ could promote the production of Cu(ɪɪɪ). The above experiments indicate that HOO$^-$ formation occurs in this system. When HOO$^-$ is present, it can complex with Cu(ɪɪ), forming Cu(ɪɪ)–OOH. The next step involves the electron transfer from the ligand to copper ions, as shown below (eqns (10)–(12)).[52] In addition, HCO$_3^-$ will be transformed into alkyl radicals, and these radicals typically exhibit strong reducing properties, capable of providing electrons to the copper ions, transitioning them from the divalent state to the monovalent state.

$$Cu(ɪɪ) + {}^•OH → Cu(ɪɪɪ) + OH^- \quad (7)$$

$$Cu(ɪɪ) + SO_4^{•-} → Cu(ɪɪɪ) + SO_4^{2-} \quad (8)$$

$$Cu(ɪɪ) + S_2O_8^{2-} → Cu(ɪɪɪ) + SO_4^{•-} + SO_4^{2-} \quad (9)$$

$$Cu(ɪɪ) + HO_2^- → [Cu(ɪɪ) – OOH]^- \quad (10)$$

$$[Cu(ɪɪ) – OOH]^- → Cu(ɪ) + HO_2^• \quad (11)$$

$$Cu(ɪ) + O_2 → Cu(ɪɪ) + O_2^{•-} \quad (12)$$
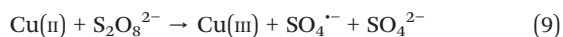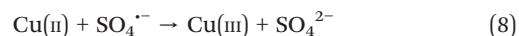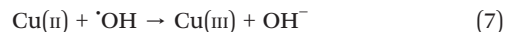
It is reported that Cu(ɪ) can react with neocuproine (NCP) through complexation, exhibiting a characteristic absorption peak at 454 nm in the PMS/Cu^{2+} system.[47] In the PDS/HCO$_3^-$/Cu^{2+} system, the same method was used to detect the presence of Cu(ɪ). Interestingly, as the reaction progresses, the absorbance at 454 nm generally increases as shown in

Table 1 The proposed degradation products of Congo red

Molecular formula	Name	m/z	Proposed structure
$C_{10}H_9N_2O_5S^-$	4-Amino-5-nitro-2,3-divinylbenzenesulfonate	269	
$C_{10}H_9NO_3S$	4-Aminonaphthalene-1-sulfonic acid	223	
$C_{12}H_{11}N$	[1,1′-Biphenyl]-4-amine	169	
$C_{12}H_{18}$	(4-Methylpentan-2-yl) benzene	162	
$C_9H_{15}N$	(2Z,5E,7E)-Nona-2,5,7-trien-1-amine	137	

Fig. 4c, indicating that Cu(I) is continuously produced during the reaction. From Fig. 4d, the copper ions still maintain a high catalytic activity after six cycles. Copper ions participate in a catalytic cycle, where they are successively oxidized and reduced, allowing them to continuously activate persulfate and generate sulfate radicals. This cycle enhances the efficiency of persulfate-based advanced oxidation processes and promotes the degradation of organic contaminants.

3.3. Optimal conditions and the effect of pH and water matrix constituents for the CR degradation

Optimal reaction conditions are determined by adjusting the concentrations of PDS and HCO_3^- as shown in Fig. S4.† From Fig. S4a,† as the concentration of PDS increased, the removal of CR increased. Combining economy and efficiency, a PDS concentration of 16 mM is considered the optimal concentration to remove CR. As shown in Fig. S4b,† without the addition of HCO_3^-, the degradation of CR can be negligible. When the amount of HCO_3^- added reaches 20 mM, CR can be degraded completely. Therefore, our next experimental conditions are: [PDS] = 16 mM, [$NaHCO_3$] = 20 mM, [CR] = 0.02 mM, and [$CuCl_2$] = 0.1 mM.

The degradation of CR is conducted under different initial pH conditions. From Fig. 5a, the sequence of CR degradation in the PDS/HCO_3^-/Cu^{2+} system is as follows: pH 8 > pH 6 > pH 10 > pH 12 > pH 2 > pH 4. It is evident that CR can be completely degraded at pH 6 and pH 8. Under strong acid conditions, the degradation of CR can be ignored. Under strong alkaline conditions, the degradation of CR can be partially inhibited. Due to the pH of the solution being around 8.2, HCO_3^- can be stable.[26] This also highlights the important role of HCO_3^- in the system. Therefore, we can conclude that the PDS/HCO_3^-/Cu^{2+} system can exhibit extremely high degradation activity under neutral, weak acid, and weak base conditions. The effects of nitrate ions (NO_3^-), sulfate ions (SO_4^{2-}), carbonate (CO_3^{2-}), dihydrogen phosphate ($H_2PO_4^-$), chloride (Cl^-), and humic acid (HA) on CR degradation by PDS/Cu^{2+}/HCO_3^- are investigated. From Fig. 5b, the presence of NO_3^-, sulfate ions (SO_4^{2-}) and

This journal is © The Royal Society of Chemistry 2024

Environ. Sci.: Water Res. Technol., 2024, **10**, 1785–1794 | **1791**

carbonate (CO_3^{2-}) has little impact on CR degradation. The addition of $H_2PO_4^-$ and HA significantly inhibits the degradation of CR, and the main reason may be that they scavenge the ROS or form complexes with copper ions.

3.4. Product analysis

First, from Fig. S5a,[1] the UV-vis spectrum shows a strong absorption peak at 500 nm, which decreases as the reaction progresses until it disappears. This indicates that the conjugated structures of CR are destroyed, leading to the cleavage of the benzene rings. Moreover, the conjugated structure of CR was further demonstrated to be destroyed by the changes in the 3D fluorescence spectra as shown in Fig. S6.† Next, Fig. S5b† exhibits the IR changes of CR after the reaction. The weak peak at 3465 cm^{-1}, corresponding to the stretching vibration of amide (NH), disappeared after the reaction. For the CR, the peak at 1583 cm^{-1} was assigned to the azo bond (N═N) and it appeared after the reaction, indicating that the azo bond could be degraded in the PDS/HCO_3^-/Cu^{2+} system.

After the reaction, the two absorption peaks observed at 1622 and 1674 cm^{-1} are likely attributed to the stretching vibrations of the carbon–carbon double bonds in the alkene molecule. In addition, the absorption peak around 1276 cm^{-1} corresponds to the bending vibration of the carbon–hydrogen (C–H) bonds. Based on the analysis above, we believe that the conjugated structure of CR has been disrupted and has undergone a ring-opening reaction. Based on the above analysis, along with the mass spectrometry results (Fig. S7†), the degradation products of CR in the PDS/HCO_3^-/Cu^{2+} system are shown in Table 1.

4. Conclusion

Our results demonstrate that the addition of bicarbonate to the persulfate-based advanced oxidation system, mediated by divalent copper ions, can strongly promote the degradation of pollutants. The introduced bicarbonate will be transformed into alkyl radicals, and these radicals typically exhibit strong reducing properties, capable of providing electrons to copper ions. This process converted the copper ions from the divalent state to the monovalent state, promoting the cycling of the different oxidation states of copper ions. The promotion of copper ion cycling by bicarbonate results in a sustained catalytic effect, enabling the continuous activation of persulfate, leading to the generation of sulfate radicals and hydroxyl radicals. This sustained catalytic activity contributes to prolonged oxidative degradation, thereby enhancing the overall efficiency of advanced oxidation processes in treating organic contaminants in natural water and wastewater. Overall, the synergistic effect between divalent copper ions, persulfate, and bicarbonate in advanced oxidation systems offers a promising approach for enhancing the degradation of organic pollutants.

Conflicts of interest

There are no conflicts to declare.

References

1 B. Petrie, R. Barden and B. Kasprzyk-Hordern, A review on emerging contaminants in wastewaters and the environment: Current knowledge, understudied areas and recommendations for future monitoring, *Water Res.*, 2015, **72**, 3–27.

2 X.-w. Ao, J. Eloranta, C.-H. Huang, D. Santoro, W.-j. Sun, Z.-d. Lu and C. Li, Peracetic acid-based advanced oxidation processes for decontamination and disinfection of water: A review, *Water Res.*, 2021, **188**, 116479.

3 H. Dai, N. Li, J. Ye, J. Zhao, X. He, X. Duan, B. Yan, G. Chen and S. Wang, Confinement boosted heterogeneous advanced oxidation processes, *Chem. Eng. J.*, 2023, **472**, 144861.

4 Y. Ding, L. Fu, X. Peng, M. Lei, C. Wang and J. Jiang, Copper catalysts for radical and nonradical persulfate based advanced oxidation processes: Certainties and uncertainties, *Chem. Eng. J.*, 2022, **427**, 131776.

5 Y. Bao, C. Lian, K. Huang, H. Yu, W. Liu, J. Zhang and M. Xing, Generating High-valent Iron-oxo ≡FeIV=O Complexes in Neutral Microenvironments through Peroxymonosulfate Activation by Zn–Fe Layered Double Hydroxides, *Angew. Chem., Int. Ed.*, 2022, **61**, 202209542.

6 F. Ghanbari and M. Moradi, Application of peroxymonosulfate and its activation methods for degradation of environmental organic pollutants: Review, *Chem. Eng. J.*, 2017, **310**, 41–62.

7 R. L. Johnson, P. G. Tratnyek and R. O. B. Johnson, Persulfate Persistence under Thermal Activation Conditions, *Environ. Sci. Technol.*, 2008, **42**, 9350–9356.

8 H. Hori, A. Yamamoto, E. Hayakawa, S. Taniyasu, N. Yamashita, S. Kutsuna, H. Kiatagawa and R. Arakawa, Efficient Decomposition of Environmentally Persistent Perfluorocarboxylic Acids by Use of Persulfate as a Photochemical Oxidant, *Environ. Sci. Technol.*, 2005, **39**, 2383–2388.

9 T. K. Lau, W. Chu and N. J. D. Graham, The Aqueous Degradation of Butylated Hydroxyanisole by UV/S2O82-: Study of Reaction Mechanisms *via* Dimerization and Mineralization, *Environ. Sci. Technol.*, 2007, **41**, 613–619.

10 H. Yang, J. Joo, E. Hong, S.-J. Park, J. Lee and C.-G. Lee, Chicken litter-derived catalyst for persulfate activation to remove acetaminophen: An organic-waste-to-wealth strategy, *Chem. Eng. J.*, 2023, **471**, 144368.

1792 | *Environ. Sci.: Water Res. Technol.*, 2024, **10**, 1785–1794

This journal is © The Royal Society of Chemistry 2024

11 C.-D. Dong, Y.-C. Lu, J.-H. Chang, T.-H. Wang, C.-W. Chen and C.-M. Hung, Enhanced persulfate degradation of PAH-contaminated sediments using magnetic carbon microspheres as the catalyst substrate, *Process Saf. Environ. Prot.*, 2019, **125**, 219–227.

12 Y. Mu, X. Liang, M. Wu, C. Li, T. Xia, K. Chen and X. Li, Utilizing blast-furnace dust as a novel persulfate catalyst for the efficient removal of petroleum contaminants from soil, *J. Cleaner Prod.*, 2024, **434**, 140112.

13 Z. Dong, C. Jiang, J. Yang, X. Zhang, W. Dai and P. Cai, Transformation of iodide by Fe(II) activated peroxydisulfate, *J. Hazard. Mater.*, 2019, **373**, 519–526.

14 Y. Tong, P. Zhou, Y. Liu, N. Wang, W. Li, F. Cheng, B. Yang, J. Liang, Y. Zhang and B. Lai, Strongly enhanced Fenton-like oxidation (Fe/peroxydisulfate) by BiOI under visible light irradiation: A novel and green strategy for Fe(III) reduction, *J. Hazard. Mater.*, 2022, **428**, 128202.

15 X. Liu, Y. Li, X. Fan, F. Zhang, G. Zhang and W. Peng, Photo-accelerated Co3+/Co2+ transformation on cobalt and phosphorus co-doped g-C3N4 for Fenton-like reaction, *J. Mater. Chem. A*, 2021, **9**, 22399–22409.

16 F. Sun, T. Chen, Z. Chu, P. Zhai, H. Liu, Q. Wang, X. Zou and D. Chen, The synergistic effect of calcite and Cu2+ on the degradation of sulfadiazine *via* PDS activation: A role of Cu(III), *Water Res.*, 2022, **219**, 118529.

17 Y. Gao, Y. Zhou, S.-Y. Pang, J. Jiang, Y.-M. Shen, Y. Song, J.-B. Duan and Q. Guo, Enhanced peroxymonosulfate activation *via* complexed Mn(II): A novel non-radical oxidation mechanism involving manganese intermediates, *Water Res.*, 2021, **193**, 116856.

18 C. S. Liu, K. Shih, C. X. Sun and F. Wang, Oxidative degradation of propachlor by ferrous and copper ion activated persulfate, *Sci. Total Environ.*, 2012, **416**, 507–512.

19 J.-Y. Li, Z.-Q. Liu, Y.-H. Cui, S.-Q. Yang, J. Gu and J. Ma, Abatement of Aromatic Contaminants from Wastewater by a Heat/Persulfate Process Based on a Polymerization Mechanism, *Environ. Sci. Technol.*, 2023, **57**(47), 18575–18585, DOI: 10.1021/acs.est.2c06137.

20 Q. Ye, H. Xu, J. Zhang, Q. Wang, P. Zhou, Y. Wang, X. Huang, X. Huo, C. Liu and J. Lu, Enhancement of peroxymonosulfate activation for antibiotics removal by nano zero valent tungsten induced Cu(II)/Cu(I) redox cycles, *Chem. Eng. J.*, 2020, **382**, 123054.

21 Z. Wang, J. Deng, Y. Peng, S. Wang, Y. Fu and Y. Liu, Hydroxylamine enhanced Cu(II)/peroxydisulfate system for diclofenac degradation: Efficiency, influence factors and mechanism, *J. Environ. Chem. Eng.*, 2022, **10**, 107200.

22 T. Li, Z. Zhao, Q. Wang, P. Xie and J. Ma, Strongly enhanced Fenton degradation of organic pollutants by cysteine: An aliphatic amino acid accelerator outweighs hydroquinone analogues, *Water Res.*, 2016, **105**, 479–486.

23 W.-G. Jeong, J.-G. Kim and K. Baek, Removal of 1,2-dichloroethane in groundwater using Fenton oxidation, *J. Hazard. Mater.*, 2022, **428**, 128253.

24 Z. Yang, X. Tan, D. Tang, J. Li and J. Ma, A tale of two metal ions: contrasting behaviors of high oxidation states of Cu and Mn in a bicarbonate–H2O2 system, *Environ. Sci.: Water Res. Technol.*, 2021, **7**, 479–486.

25 M. Jiang, J. Lu, Y. Ji and D. Kong, Bicarbonate-activated persulfate oxidation of acetaminophen, *Water Res.*, 2017, **116**, 324–331.

26 L. Zhou, W. Song, Z. Chen and G. Yin, Degradation of Organic Pollutants in Wastewater by Bicarbonate-Activated Hydrogen Peroxide with a Supported Cobalt Catalyst, *Environ. Sci. Technol.*, 2013, **47**, 3833–3839.

27 B. Liu, Y. Li and S. Xing, Insight into the mechanism of CuO activated persulfate with the assistance of bicarbonate for removing organic pollutants, *J. Water Process Eng.*, 2020, **37**, 101403.

28 J. Kim, J. Wang, D. C. Ashley, V. K. Sharma and C.-H. Huang, Enhanced Degradation of Micropollutants in a Peracetic Acid–Fe(III) System with Picolinic Acid, *Environ. Sci. Technol.*, 2022, **56**, 4437–4446.

29 Y. Zhao, R. Zhang, J. Huang, Y. Zhang, B. Han, Y. Ying, M. Chen, S. Xie and D. Chen, Imprinting defective Fe-based metal-organic frameworks as an excellent platform for selective fenton/persulfate degradation of LEX: Removal performance and mechanism, *Appl. Catal., B*, 2023, **337**, 122919.

30 Q. Ye, Q. Song, J. Zhou, Y. Wu, Y. Zhou, J. Zhang and W. Wu, Behavior and fate of short chain chlorinated paraffins (SCCPs) in different oxidation reactions, *Chem. Eng. J.*, 2023, **464**, 142557.

31 L. Wang, D. Luo, J. Yang and C. Wang, Metal-organic frameworks-derived catalysts for contaminant degradation in persulfate-based advanced oxidation processes, *J. Cleaner Prod.*, 2022, **375**, 134118.

32 O. S. Furman, A. L. Teel and R. J. Watts, Mechanism of Base Activation of Persulfate, *Environ. Sci. Technol.*, 2010, **44**, 6423–6428.

33 W.-D. Oh, Z. Dong and T.-T. Lim, Generation of sulfate radical through heterogeneous catalysis for organic contaminants removal: Current development, challenges and prospects, *Appl. Catal., B*, 2016, **194**, 169–201.

34 C. Liang, C.-F. Huang, N. Mohanty and R. M. Kurakalva, A rapid spectrophotometric determination of persulfate anion in ISCO, *Chemosphere*, 2008, **73**, 1540–1543.

35 H. Liu, J. Zhao, Y. Wang, Y. Wu, W. Dong, M. Nie and X. Wang, Enhancement of peroxymonosulfate activation by sinapic acid accelerating Fe(III)/Fe(II) cycle, *Chem. Eng. J.*, 2022, **446**, 137177.

36 X. Cheng, H. Guo, Y. Zhang, X. Wu and Y. Liu, Non-photochemical production of singlet oxygen *via* activation of persulfate by carbon nanotubes, *Water Res.*, 2017, **113**, 80–88.

37 D. Huang, W. Xu, L. Lei, S. Chen, C. Lai, W. Zhou, Y. Chen and R. Li, Promoted generation strategies and corresponding roles of singlet oxygen in activation of persulfate by nanoscale zero-valent iron systems, *Chem. Eng. J.*, 2022, **449**, 137493.

38 Q. Wang, B. Wang, Y. Ma and S. Xing, Enhanced superoxide radical production for ofloxacin removal *via* persulfate

This journal is © The Royal Society of Chemistry 2024

Environ. Sci.: Water Res. Technol., 2024, **10**, 1785–1794 | **1793**

activation with Cu-Fe oxide, *Chem. Eng. J.*, 2018, **354**, 473–480.

39 S. Zhu, X. Li, J. Kang, X. Duan and S. Wang, Persulfate Activation on Crystallographic Manganese Oxides: Mechanism of Singlet Oxygen Evolution for Nonradical Selective Degradation of Aqueous Contaminants, *Environ. Sci. Technol.*, 2019, **53**, 307–315.

40 L. Wang, K. Xiao and H. Zhao, The debatable role of singlet oxygen in persulfate-based advanced oxidation processes, *Water Res.*, 2023, **235**, 119925.

41 A. A. Gorman and M. A. J. Rodgers, Singlet molecular oxygen, *Chem. Soc. Rev.*, 1981, **10**, 205–231.

42 H. Li, C. Shan and B. Pan, Fe(III)-Doped g-C3N4 Mediated Peroxymonosulfate Activation for Selective Degradation of Phenolic Compounds *via* High-Valent Iron-Oxo Species, *Environ. Sci. Technol.*, 2018, **52**, 2197–2205.

43 Z. Fang, J. Zhao, Y. Li, Y. Wang, T. Qiu, Y. Wu, W. Dong and G. Mailhot, Improving Fenton-like system with Catechin, an environmental-friendly polyphenol: Effects and mechanism, *Chem. Eng. J.*, 2021, **426**, 127946.

44 D. Li, C. Pan, Y. Zong, D. Wu, Y. Ding, C. Wang, S. Wang and J. C. Crittenden, Ru(III)-Periodate for High Performance and Selective Degradation of Aqueous Organic Pollutants: Important Role of Ru(V) and Ru(IV), *Environ. Sci. Technol.*, 2023, **57**, 12094–12104.

45 C. Chen, Y. Wang, Y. Huang, J. Hua, W. Qu, D. Xia, C. He, V. K. Sharma and D. Shu, Overlooked self-catalytic mechanism in phenolic moiety-mediated Fenton-like system: Formation of Fe(III) hydroperoxide complex and co-treatment of refractory pollutants, *Appl. Catal., B*, 2023, **321**, 122062.

46 A. Kottapurath Vijay, V. K. Sharma and D. Meyerstein, Overlooked Formation of Carbonate Radical Anions in the Oxidation of Iron(II) by Oxygen in the Presence of Bicarbonate, *Angew. Chem., Int. Ed.*, 2023, **62**, e202309472.

47 L. Wang, H. Xu, N. Jiang, Z. Wang, J. Jiang and T. Zhang, Trace Cupric Species Triggered Decomposition of Peroxymonosulfate and Degradation of Organic Pollutants: Cu(III) Being the Primary and Selective Intermediate Oxidant, *Environ. Sci. Technol.*, 2020, **54**, 4686–4694.

48 Y. Feng, P.-H. Lee, D. Wu, Z. Zhou, H. Li and K. Shih, Degradation of contaminants by Cu+−activated molecular oxygen in aqueous solutions: Evidence for cupryl species (Cu3+), *J. Hazard. Mater.*, 2017, **331**, 81–87.

49 R. L. Frost, W. Martens, J. T. Kloprogge and P. A. Williams, Raman spectroscopy of the basic copper chloride minerals atacamite and paratacamite: implications for the study of copper, brass and bronze objects of archaeological significance, *J. Raman Spectrosc.*, 2002, **33**, 801–806.

50 J. Chen, X. Zhou, P. Sun, Y. Zhang and C.-H. Huang, Complexation Enhances Cu(II)-Activated Peroxydisulfate: A Novel Activation Mechanism and Cu(III) Contribution, *Environ. Sci. Technol.*, 2019, **53**, 11774–11782.

51 A. Balikungeri, M. Pelletier and D. Monnier, Contribution to the study of the complexes bis(dihydrogen tellurato)cuprate(III) and argentate(III), bis(hydrogen periodato)cuprate(III) and argentate(III), *Inorg. Chim. Acta*, 1977, **22**, 7–14.

52 H.-J. Lee, H. Lee and C. Lee, Degradation of diclofenac and carbamazepine by the copper(II)-catalyzed dark and photo-assisted Fenton-like systems, *Chem. Eng. J.*, 2014, **245**, 258–264.